T.C.

ISTANBUL AYDIN UNIVERSITY

INSTITUTE OF GRADUATE STUDIES

HYBRID STORAGE SYSTEM TO COPE WITH FLUCTUATING POWER OF HYBRID RENEWABLE ENERGY-BASED SYSTEMS

MASTER'S THESIS

YAHYA ABU ATTEIEH

Department of Electrical and Electronics Engineering

Electrical and Electronics Engineering Program

December, 2022

T.C.
ISTANBUL AYDIN UNIVERSITY
INSTITUTE OF GRADUATE STUDIES

HYBRID STORAGE SYSTEM TO COPE WITH FLUCTUATING POWER OF HYBRID RENEWABLE ENERGY-BASED SYSTEMS

MASTER'S THESIS

YAHYA ABU ATTEIEH
(Y2013300010)

Department of Electrical and Electronics Engineering
Electrical and Electronics Engineering Program

Thesis Advisor: Prof. Dr. MURTAZA FARSADI

December, 2022

APPROVAL PAGE

DECLARATION

I hereby declare with respect that the study “Hybrid Storage System To Cope With Fluctuating Power Of Hybrid Renewable Energy-Based Systems”, which I submitted as a Master thesis, is written without any assistance in violation of scientific ethics and traditions in all the processes from the Project phase to the conclusion of the thesis and that the works I have benefited are from those shown in the Bibliography. (.../.../20...)

YAHYA ABU ATTEIEH

FOREWORD

In the beginning I would like to thank my mother and father, My Ideals who raised me to be the good person I'm today, for being patient, loving and supporting through it all. I hope one day I can return some of what they gave me, everything I have accomplished is because of them.

I would like to express my gratitude to my advisor prof. Dr. MURTAZA FARSADI for his guidance and encouragement, the suggestions and comments during the making of this thesis. I'm truly grateful for working with him all this time.

Finally, I would like to thank my friends for always believing in me and encouraging me from day one.

JULY , 2022 YAHYA ABU ATTEIEH

HYBRID STORAGE SYSTEM TO COPE WITH FLUCTUATING POWER OF HYBRID RENEWABLE ENERGY-BASED SYSTEMS

ABSTRACT

In order to deal with the reduced power density of the battery, researchers extensively explore supercapacitor technology. A hybrid battery-supercapacitor storage (HBSS) design may boost overall efficiency by combining the higher energy density of the battery with the higher power density of the supercapacitor. This hybrid storage approach has been the subject of ongoing research in the electric vehicle (EV) sector; In order to solve the non-dispatchability of wind and solar energy, it is now undergoing trial installation in the power system. Three high power loads were used to model the system in this paper's supercapacitor to examine how it would effect the whole setup and how the supercapacitor would handle the fluctuating voltage.

Keywords: HBSS hybrid battery super capacitor storage system , non-dispatchability

HİBRİT YENİLENEBİLİR ENERJİ TABANLI SİSTEMLERİN DALGALANAN GÜCÜYLE BAŞA ÇIKMAK İÇİN HİBRİT DEPOLAMA ÇERÇEVESİ

ÖZET

Yenilenebilir enerji sıklıkla şebeke için elektrik üretmek ve bağımsız ekipmana güç sağlamak için kullanılır. Enerji, iş yapabilme kapasitesi olarak tanımlanır ve yaşayan her süreç için önemlidir. Enerji asla kaybolmaz ama birçok forma dönüşebilir. Yenilenebilir enerji kaynaklarını kullanmanın olumlu yanı, füzel yakıtı kullanımını azaltmak; Bu tezde, sistemimizi yükledikten sonra güç oranının verimliliğini tespit etmemize rağmen, bir süper kapasitör kullanarak gücün kapasitesini artırmayı amaçlıyoruz. Düzensiz elektrik profillerine sahip bağımsız mikro şebekelerde, bir kurşun-asit batarya enerji depolama sistemini (ESS) süper kapasitörlerle hibritleştirmek, artan batarya bozulmasıyla başa çıkmak için uygun bir seçenektir. Sağlanan gücün güvenilirliğini artırmak için, bir güneş enerjisi sisteminde bir süper kapasitör-batarya hibrit enerji depolama sistemi kullanılır.

Anahtar Kelimeler: ESS) süper kapasitörlerle hibritleştirmek

TABLE OF CONTENT

ABBREVIATIONS

(HBSS)	**:**	hybrid battery-supercapacitor storage
(IIR)	**:**	filters and infinite impulse response
ADALINE	**:**	Adaptive Linear Element
APF	**:**	Active Power Filters
CBF	**:**	Complex Band-pass Filter
CC	**:**	Continuous Conduction
ESSs	**:**	energy storage systems
FC	**:**	Fundamental Contituent
FF	**:**	Fundamental Frequency
FIR	**:**	finite impulse response
HSS	**:**	hybrid storage system
ICN	**:**	Incremental Conductance
ILF	**:**	In-loop Filter
LPF	**:**	low pass filter
MPPT	**:**	Maximum Power Point Tracker
MROGI	**:**	Modified Reduced Order Generalized Integrator
P&O	**:**	Pertube and Observe
PF	**:**	Passive Filters
PV	**:**	Photo Voltaic Panel
PWM	**:**	Pulse With Modulation
SPWM	**:**	Sinusoidal Pulse With Modulation
SRF	**:**	Synchronous Reference Frame

LIST OF TABLES

LIST OF FIGURES

I. INTRODUCTION

A. Renewable energy:

Renewable energy is an umbrella term defined as a broad spectrum of resources that renews their energy source on their own. Renewable energy sources are a group of natural materials that do not run out or pollute the environment, such as the sun, wind, and water.

Rising concern over environmental awareness, climate change impacts, and sustainability derived the interest in reforming energy.

Researchers, governments, policymakers, academics, and other interested parties invested in researching and transitioning toward sustainable energy and its use in every sector and household. Innovation and technology are the new trendy topics of the last few decades, and the world has combined technology and nature to build sustainable, innovative communities. For example, the European Union pushes its vision of renewable energy technologies with its citizens, where citizens participate actively in taking ownership of energy transition.

II. LITERATURE REVIEW

Modern technology's need on electricity is essential for its unrelenting advancement. The gap between the demand for and supply of electrical energy is widening as electrical energy use spreads around the globe. Since fossil fuels are becoming more expensive, emphasis has been placed on using renewable energy as a substitute for producing electricity. The various applications of sun and wind energy sources are in desire for power generation because they also address issues like the year-round unavailability of solar or wind power due to their unproductive nature by using hybrid renewable energy instead of focusing on any one source (solar or wind or biomass) and become cost-effective by lowering unit cost of generation. In order to optimize a standalone solar-wind hybrid power generating system and maximize the usage of renewable energy resources while lowering the system's overall tariff, this paper's major goal is to reflect the neutral viewpoints of many writers. The HOMER system was optimized year-round while taking into account various system costs, the amount of renewable energy used, carbon emissions, and electrical load requirementsSupercapacitors are used in situations that call for many quick charge/discharge cycles rather than long-term compact energy storage.

1. PV system Constituents

The photovoltaic effect is illustrated in Figure 2.1. Sunlight, made up of photons that carry a specific amount of energy, hits a solar array and produces an electric current. A solar battery consists of the connection of each solar panel with a small amount of electricity. [**WEIDONG XIAO 2017**]. The DC-DC power is produced by solar arrary. Consequently, to change from DC to AC, an inverter is needed, and that’s for solar energy utilization. The AC electricity produced by the inverter can be used locally to power equipment or sent to the grid somewhere else. [**WEIDONG XIAO 2017**].

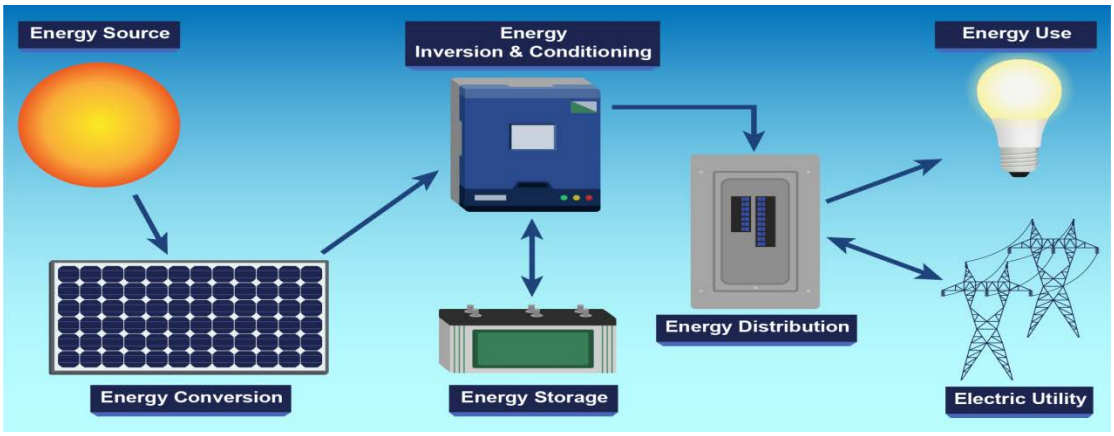

Figure 1. PV model

The PV system was made up of a [Cel l, Modu le, Pan el, Stri ng, Suba rray, Arr ay]. The P - V cel l, which is surprisingly named a photovoltaic cel l too, is the basic building block of a P - V powe r grid. As seen in figure 2.2, a solar cell with a crystalline basis provides a contact. Melting, doping, metallization, and texturing are all components of the production process. One contact cell's DC voltage, which is less than one V when measured between the positive and negative sides of the junction, is too low for many real-world uses. Furthermore, due to its fragile nature by nature, it has to be shielded and covered with a protective coating before use. [**WEIDONG XIAO 2017**]

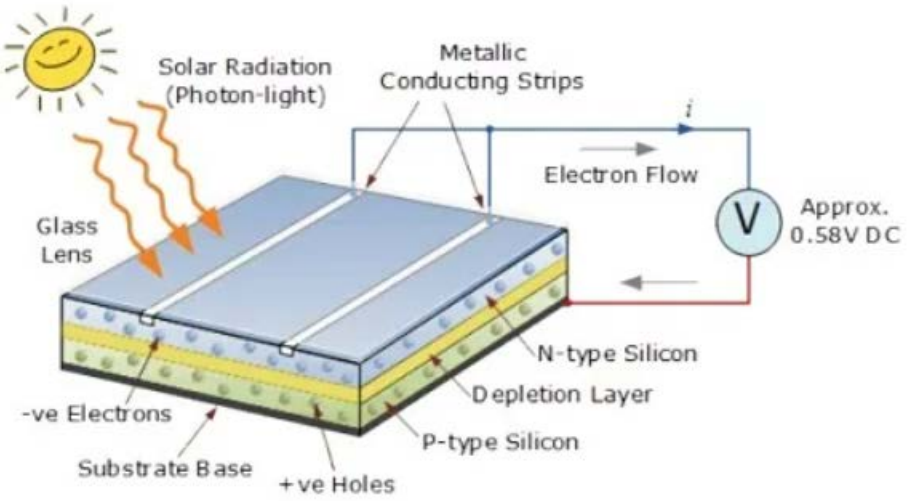

Figure 2. Solar cell

larger voltages and power than a single cell may be produced by the photovoltaic system or sol ar pane l., is the most important component for end consumers. A covering of protection and connections hold the PV module's cells together. Thanks to grid-connected installations and advancements in power-

conditioning equipment, the number of cells in a P - V module is no longer limited by the nominal voltages of batteries or mass.. PV cells with crystalline structures are sandwiched between two sheets of substrate and superstrate to form a PV panel. [**WEIDONG XIAO 2017**]

Tempered glass serves as a superstrate that protects sensitive cells and aids with module coverage. Since each area unit in glass is made of a semiconductor, it has a quantifiable connection of thermal growth that is identical to that of a crystalline PV cell. Tempered glass has roughly 94 light transmissions and is strong and transparent. The glass's surface is not perfectly smooth to reduce light reflections. PV cells are connected in series using metal conductors that go from the surface to the lowest point. The PV cells are protected by an encapsulate, which is a substance that sits between the superstrate and the substrate and encloses the PV cells. [**WEIDONG XIAO 2017**]

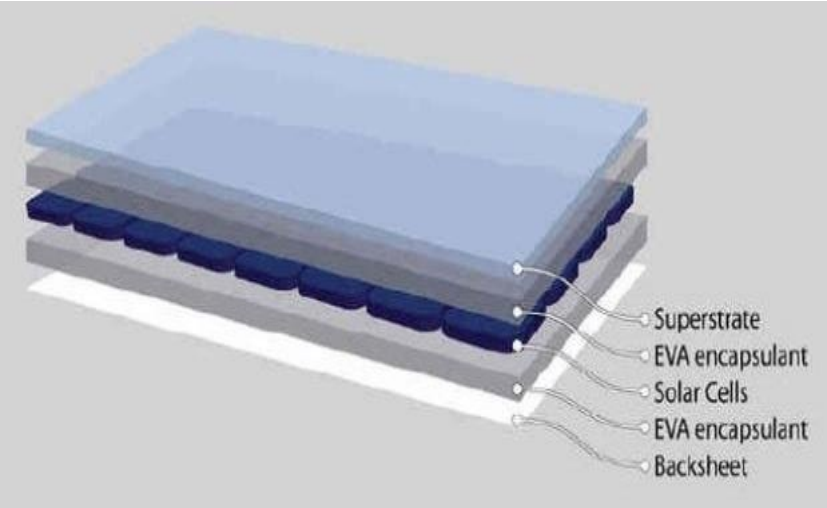

Figure 3. Inside solar

A submodule consists of 3 divisions that is formed by the connection of 72 cells linked in series. In addition to that, 24-star cells are associated in parallel to the submodules that has single bypass diode. In case the cell in the system produces an imbalanced power, then directly the implementation expels the negative effect of the hot spots. This implementation is shown in figure 1.1.4.

To guarantee an environmentally protected item, the AC modules is built from different lamination parts with the star cells, junction box, electric connectors, and substrate. This Module is a substitute for the PV modules, thus there has to be more attention on it.

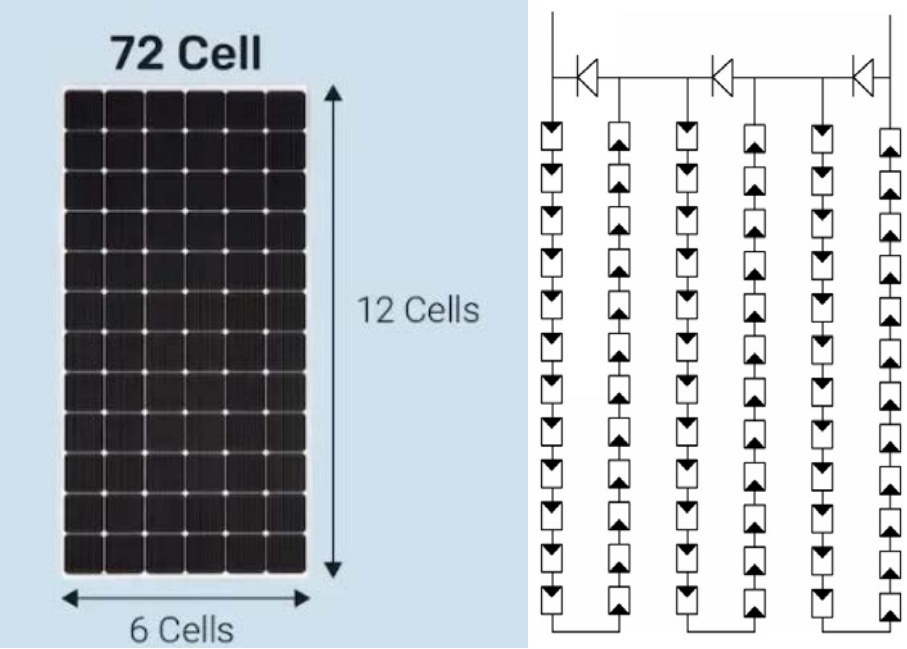

Figure 4. 72 cell

It's essential to use some terminology while discussing PV generators. The progression of the ability capacity from the cell level to the array level is illustrated in Figure 2.5. PV power systems are often formed using nonparallel and/or parallel PV module designs. The term "stringing" is frequently used to describe connecting star modules in order to raise output voltage. By connecting them in parallel, it is feasible to build a collection of PV strings that can produce hundreds or even millions of watts. Large solar power facilities employ several subarrays. [**WEIDONG XIAO 2017**] A monopolar array or subarray has two wires in its output circuit, one of which is positive (+) and the other is negative (-). (-). Two monopolar subarrays combine to make a PV array with two poles with a function that is neutral, as in “Fi.g 1.1.4”. To force the power and voltage ratios of the twin monopolar subarrays to coincide would be excellent. According to studies, For large-scale P - V power systems and bipolar array topologies, E Energy is the market leader in producing utility-interaction inverters. The inverter controls the output of the bipolar P - V array., which has a maximum voltage rating of +600 V.

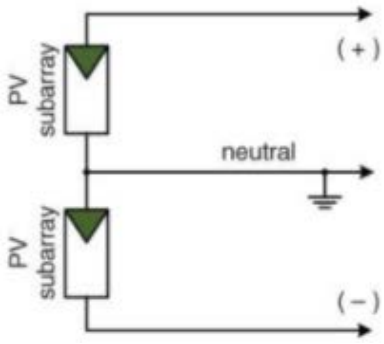

Figure 5. PV subarray

2. P - V Out put Characteristics

Curves of currnt – voltag and power-voltage often serve as visual representations of the output of P - V cells and modules. The properties of the P - V output under certain circumstances may also be shown by these graphs.such as when a battery is involved. Current-voltage , power voltage graphs for a P V cell's output are in fig 1.2. These graphs may be used for various devices. After the star cells have been tested under similar conditions, a PV module, string, or array may be represented by normalized curves. Figures depict the four crucial values and three critical points specified in Table 2.1. Some data is included in the data set to account for the nominal rating. [**WEIDONG XIAO 2017**]

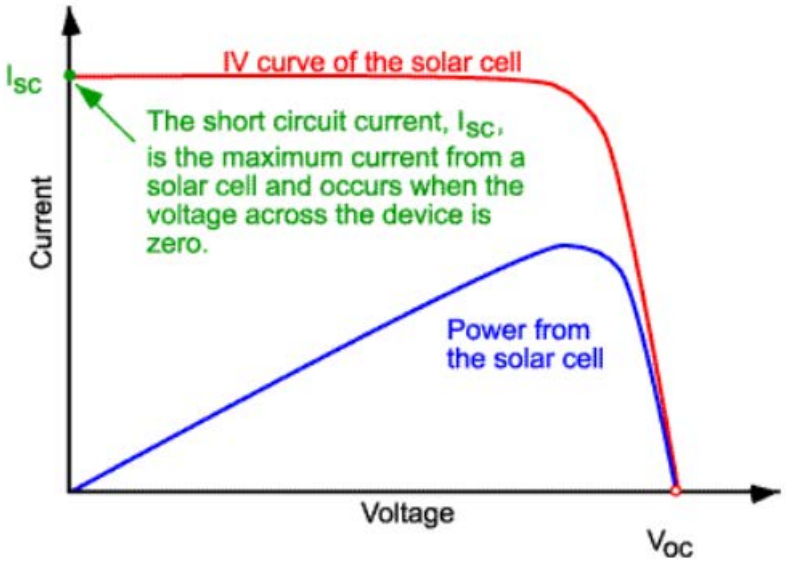

Figure 6.IV curve

Table 1.Symbol Describtion

Symbol	Description
V_{OC}	When the PV output terminal is open-circuit and exhibiting zero current, the open-circuit voltage is monitored.
I_{SC}	When the PV generator terminal is short-circuited, the short-circuit current is measured.
I_{MPP}	At the MPP, the current is measured.
V_{MPP}	At the MPP, the voltage is measured.

Pmaxpp=Vmaxpp*Imaxpp

To determine instantaneous maximum power point (MPP), MPPT is needed which dependen on the cell temperature, solar irridiation and other variables.

3. Standalone System

In the 1950s, hundreds of people in rural areas received electricity from PV systems only because it was a standard technology used for domestic power supply. Radiation is more significant inside because of the atmosphere and clouds. The optimal environment for solar power production is regarded as being outside. Satellites, spaceships, housing stations, rural residences, towns, streetlights, communication nodes, pumping systems, and automobiles are a few examples of independent systems. [**W. Parker 2016**] In order to accommodate the intermittent nature of solar energy output, the utility grid plays a significant part in large-scale solar energy production. Grid-connected P - V systems are now constructed in areas where grid conn. are not practical. Independent P - V systems may provide direct current, alternative current, or both forms of electricity, depending on the situation. Despite the absence of massive energy storage, PV producers may nevertheless provide hundreds of kilowatts of electricity either directly or via power interfaces. Equipment for power conditioning may be used in systems that are connected indirectly and need voltage conversion. Due to the intermittent nature of solar power production, the bulk of applications need for energy storage. A hybrid system may be powered by ordinary engines, fuel cells, or even wind turbines, as illustrated in Figure 1.3. [**A. ElMehdi 2016**]

Since the energy storage is just a buffer and not a power supply, a P - V-battery system is not a hybrid system in the absence of other resources. BOS is made up of several parts, such as facilitysources. The battery bank must almost constantly

be charged using charge controllers.Despite the fact that they are required, Figure 1.3 depicts BOS without filters or other security measures. [**A. ElMehdi 2016**]

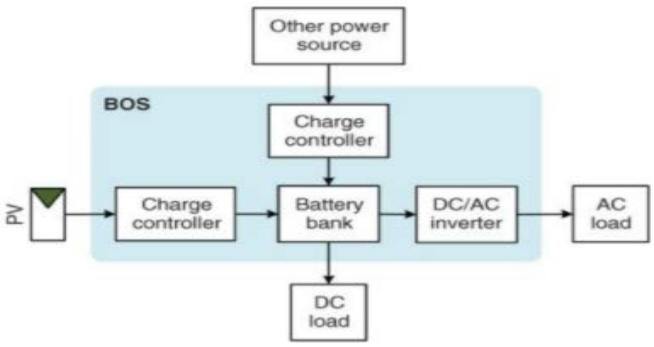

Figure 7. Power generation of PV panel

B. DC Grid and Micro grid Connections

For AC grids, grid association is more important. Microgrids and DC distribution systems have gained popularity and continue to demonstrate their ability to compete with traditional AC grids.

all over the place. The use of HVDC systems for transporting huge quantities of power across long distances has been demonstrated in a number of locations throughout the globe. Low tension applications are another advantage of DC. Electronic devices including printers, monitors, laptops, and phones may operate directly off of direct current (D - C) power supply. Modern data centers considerably reduce power usage by using standardized and extensible D - C power sources. Previous versions of induction and magnet synchronous motors used three-phase A - C electricity. DC variable-speed drives are essential as a result of recent developments in power physics and management engineering. Thanks to DC power sources, the motor runs effectively, smoothly, and inexpensively. Due to the existing AC supply system, a two-stage transition from alternative to direct to alternative current is often required for many applications, even though this causes significant losses. LVDC and HVDC have both shown success in industrial settings. The potential advantages of medium-voltage DC systems over more conventional medium-voltage AC systems are still being studied, despite the fact that they are not discussed as often as HVDC and LVDC systems. [**WEIDONG XIAO 2017**]

Figure 2 is an example of an LVDC micro grid. The system connects two DC distribution panels using a standard DC bus. To accommodate a variety of power

sources and loads, the system makes use of standardized DC buses. Connecting is simpler than in an A - C system since the only variable that has to be handled is the D - C voltage. For any electromagnetic device, a variety of well-managed power-conditioning circuits are available. MPPT mode is widely utilized on the DC/DC power interfaces to increase the quantity of solar energy produced by PV generators.

In order to balance generation and freight, battery storage systems are employed. DC bus voltage is managed by managing the charging and draining of battery modules. The only time PV power production will be permitted to cease is when it exceeds all loads and the MPP battery. An urban or suburban design may help with resource and freight cooperation. The "droop method" is a well-known formula for the decentralized administration and coordination of various sharing systems. The AC grid may also be connected using duplex DC/AC converters. [**WEIDONG XIAO 2017**].

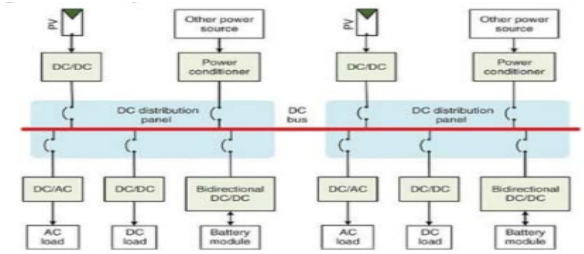

Figure 8. D C micro grid

1. MaximumPowerPointTracking (M. P. P. T.)

For their first sensible cell, which was awarded a patent in 1954, Fuller and his colleagues scientists received a prize. A PV module may now be linked to a dynamic load, such as a DC motor, as in Fig. 2.1.2, or a resistive load, such as a DC light, depending on the module's intended use. Where the module and cargo -V curves overlap is where the module's operating function is located., Despite the fact that there is only one most electrical outlet (MPP) on the module l-V curve and it is non-linear, When the module/array is partially shaded, as in Fig. 2.1.3, the P.V curve contains several peaks, which shows that the M. P. P has been moved. [**S. Kim**]

In an attempt to boost the power and effectiveness of PV systems, researchers have been researching the most electrical outlet chase (MPPT) since 1954.

Electrical trackers and mechanical single- and dual-axis trackers are the two main types of MPTs. You may direct the P - V module to track the sun by using a

"suntracker," often known as a motorized huntsman. But this method of deployment is costly, time-consuming, and ineffective. Scientists have concentrated their efforts in search of electricity.The three electrical MPPT approach categories are as follows: Techniques used offline, such as aliquot ope n - circuit (FOCV) and aliquot shor t - circuit (ASC).

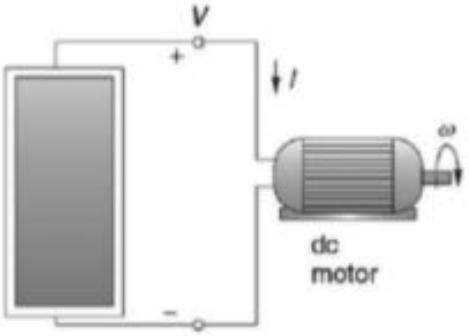

Figure 9. P - V module coupled with a dynamic load

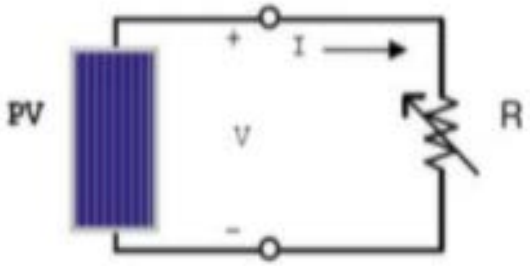

Figure 10. A solar panel coupled to a resistive load (R)

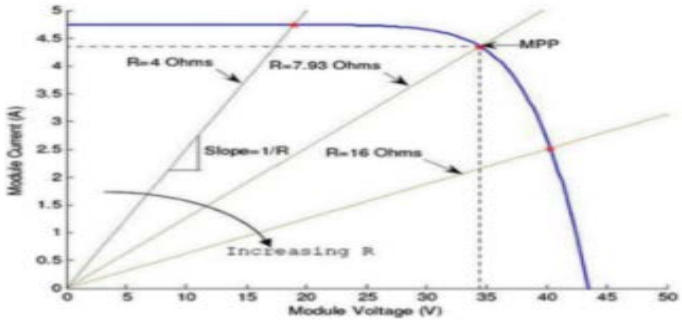

Figure 11.Placement of the operational point in relation to load resistance (R)

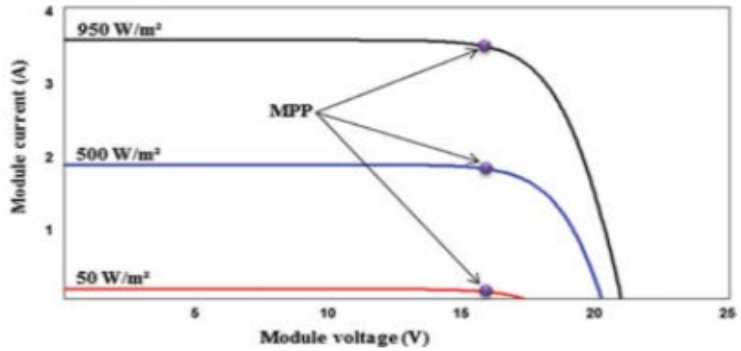

Figure 12. Irradiation level's effect on MPP location

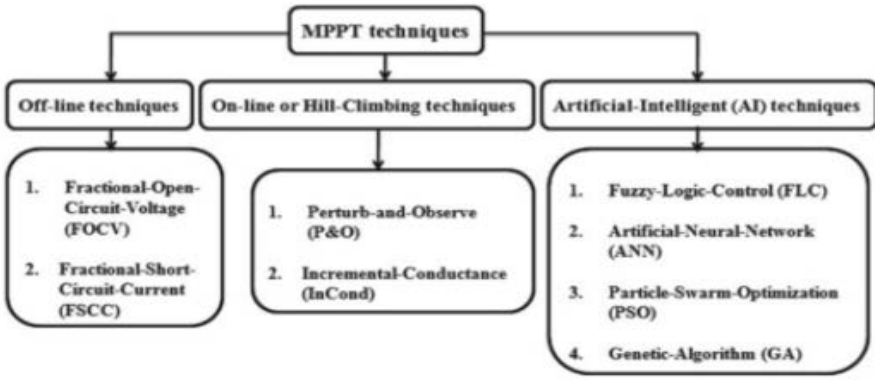

Figure 13. Max power point tracking tech.

Between 1954 and 2018, several techniques and advancements were described in the scientific literature. Every MPPT research carried out before to 1988 employed a module or load to guarantee that the cargo current-voltage specification curves and module were near to and practical with respect to the MPP. In order to improve the compatibility between the characteristics of the module and the cargo under a range of irradiation levels and near temperatures, several studies were conducted at the time to determine the best battery requirements to connect to the PV system. The MPP was investigated by Hooke et al. in 1961 to determine where the current - voltage curves of a resistive load and a module cross. A 1976 experiment by Brian and colleagues found that the MPP is the location where a module's current - voltage curve and its dynamic load overlap. According to Braunstein's 1977 study, the MPP is the point when the current-voltage curves for the modul and batteryload converge. his style study from 1977, Appelbaum solely considered resistive loads and storage. [**Ali M.**].

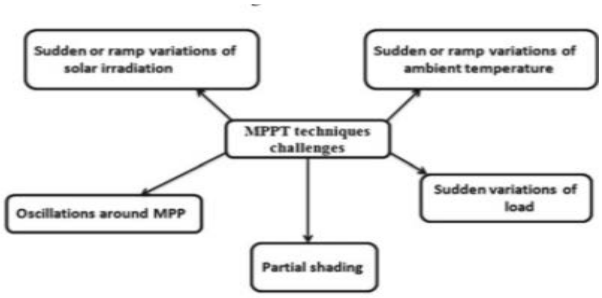

Figure 14. Challenges facing MPPT techniques

The MPPT controller is frequently implemented using entirely unique methods and algorithms. Perturb and Observe (P&O) and progressive electrical phenomena are the two most used methods (INC). [**Nabil Derbel 2018**]

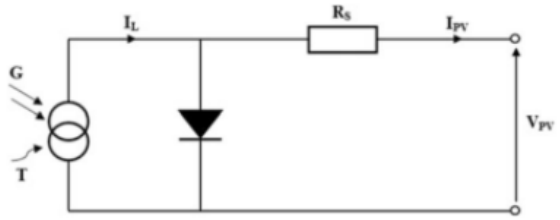

Fig. 1.1 Equivalent model of PV cell

Figure 15. Equivalent of PV cell

2. DC voltage control

Fig. 2.2.1 depicts the whole system. The main D C / D C converter may be regulated using an MPPT algorithm to ensure that the lower PV power might grow to its maximum level under a variety of climatic variables. The second D - C / D - C conv. may elevate the input voltage to level needed by the VS, which has a harsh and rapid duty cycle, and act as a second D C / D C converter. [**Nabil Derbel 2018**]

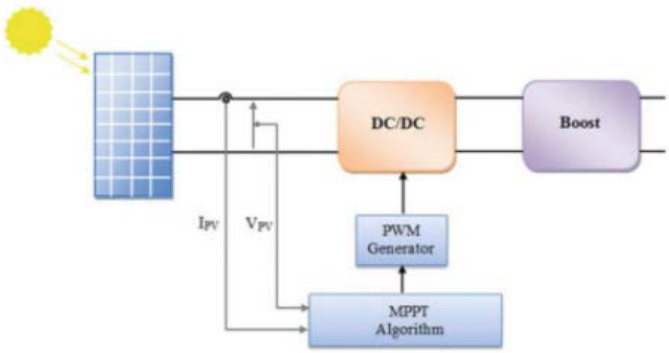

Figure 16. D C - V regulation

3. Pulse With Modulation Regulation

A three-phase DC-to-AC converter makes up this invariant. The complex

electrical inverter circuit is shown in Figure 2.3. The electrical inverter's three arms each have one or two switches in them. A diode is connected in parallel with the semiconductor component (IGBT, MOSFET...). The pulse-width modulation (PWM) inverters' high-order harmonics are reduced by the L-C filter, which is connected to the electrical converter's output. [**Nabil Derbel**]

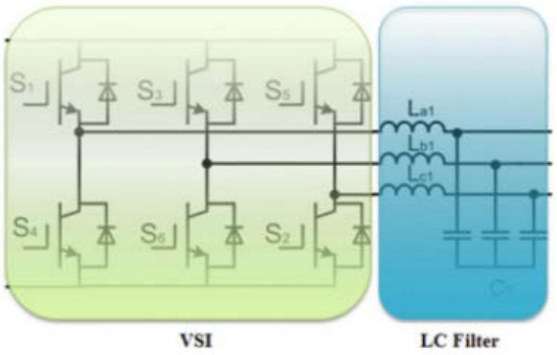

Figure 17. Three-phase VSI

Pulsewidthmodulation is a technique for generating an analogsignal from a digitalsource (PWM).Duty cycle and frequency work together to control how PWM signals behave. PWM may convert a set DC voltage to a variable DC voltage. THD (Total Harmonic Distortion) may be reduced by using PWM. It is important to take distortion into consideration and filter a PWM inverter's output while trying to meet the THD requirement. The most well-known PWM modulation techniques are sinusoidal, hysteretic, space vector, and optimum modulation. The SPWM controls the inverter switching in this system. To create SPWM and generate the gating signal for the transistors illustrated in Figure 2.3.3, the highfrequency triangularcarrier wave VCR is compared to a sinusoidal frequency reference Vm. [**Nabil Derbel 2018**]

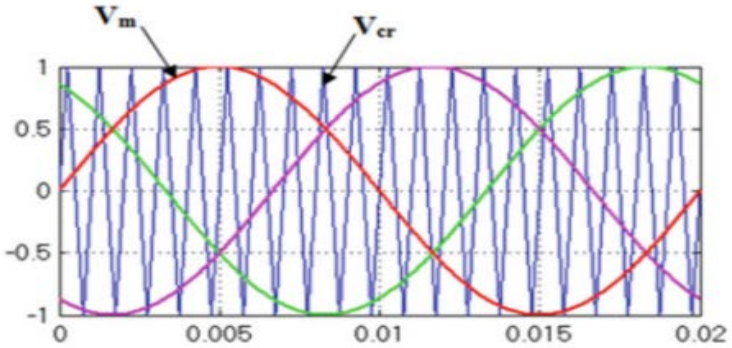

Figure 18. Reference voltage and triangle wave carrier

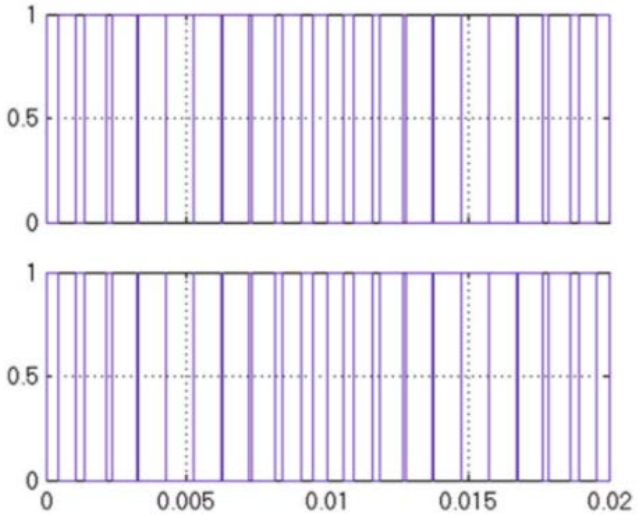

Figure 19.The inverter's first arm receives a pulse from the generator.

III. WIND TOURBINE:

A. Work function:

Over the last 2000 years, windmills have helped people harness the energy of the wind and convert it into a variety of useful forms. The quantity of wind energy that can be converted into electricity by modern wind turbines is significant.. This is as a result of the blades' development using sophisticated aerodynamic research and other methods that boost performance. Let's investigate its basic functionality.

If the wind can turn, the generator attached to the wing will provide us with electricity.

But how does the wind cause the wing to turn?

From the root to the tip of the Blade, there are different sizes and shapes of airfoil cross sections.

The fundamental airfoil principle is what makes the wind turbine blades revolve. Fluid passing across an airfol creates a lift force.The wind turbine generates the fundamental rotation that we are used to witnessing in this way. Similar to how you would on a moving train, the spinning Blade of a wind turbine feels the wind relative to it—the relative wind speed for the Blade in motion. Therefore, the relative wind speed and the wind turbine blade are both angled. The relative windspeed is increasingly inclined to the tip as the blade velocity increases near the tip. The Blade is clearly continually twisted from root to tip, according to this. On the other hand, a generator cannot be connected directly to this spin. Due to problems with noise and mechanical strength, wind turbine blades usually spin at relatively low revolutions per minute (rpm).

This rule rotational velocity makes it impossible for a generator to produce the proper electrical frequency. In order to connect to the generator, a gearbox increases speed.

The gearbox achieves a high-speed ratio using a planetary gear set

arrangement.

There is a break within the nacelle as well. The brake's function is to stop the wind blades from rotating when there is too much wind.

As a consequence, the base, which contains a step-up transformer, receives the power that flows through the lines. For maximum power extraction, the wind turbine should face the direction of the wind. The wind's direction is erratic, however. The windspeed & direction are measured via a velocity sensor that is mounted on top of the nacelle.The wind's direction deviation is detected by an electronic controller, which then makes use of it to provide the correct signal to the yawing mechanism and correct the error. The nacelle's rotation by the yaw motors is visible. The wind turbine will thus face the wind's direction at all times: Along with wind speed, the relative velocity angle of the wind also fluctuates. By tilting the blades, a blade tilting mechanism makes sure that the Blade is properly aligned with the relative velocity. The blades continually attack the wind at their optimal angle as a consequence.

The effectiveness of the wind turbine is a very intriguing topic. assuming that the wind speed is monitored both upstream and downstream of the wind turbine in order to fully comprehend the wind turbine's efficiency. As can be observed, the upstream wind speed is much higher than the downstream wind speed. This is as a result of the blades partly absorbing the kinetic energy of the wind.

The wind turbine produces mechanical power from the same amount of energy. Wind turbines only use kinetic energy when the downstream wind speed is zero. However, according to the principles of physics, a condition with zero downstream wind speed is impossible. In other words, a downstream speed of 0 indicates a stock-flow all the way through. It is required to have a specified amount of exit wind speed because of the flow's physical needs. In other words, a wind turbine is capable of reaching its maximum degree of efficiency in theory.

This limitation is referred to as Betz's limit.

In essence, it means that no wind turbine will ever be able to achieve an efficiency level higher than 59.3 percent.

Pmec is equal to 12 mVIN2 - 12 mVout2 VoutVin.

Speed ratio: 1:90 Cutoff speed: 80 km/hr Vrelative: Vwind-Vblade

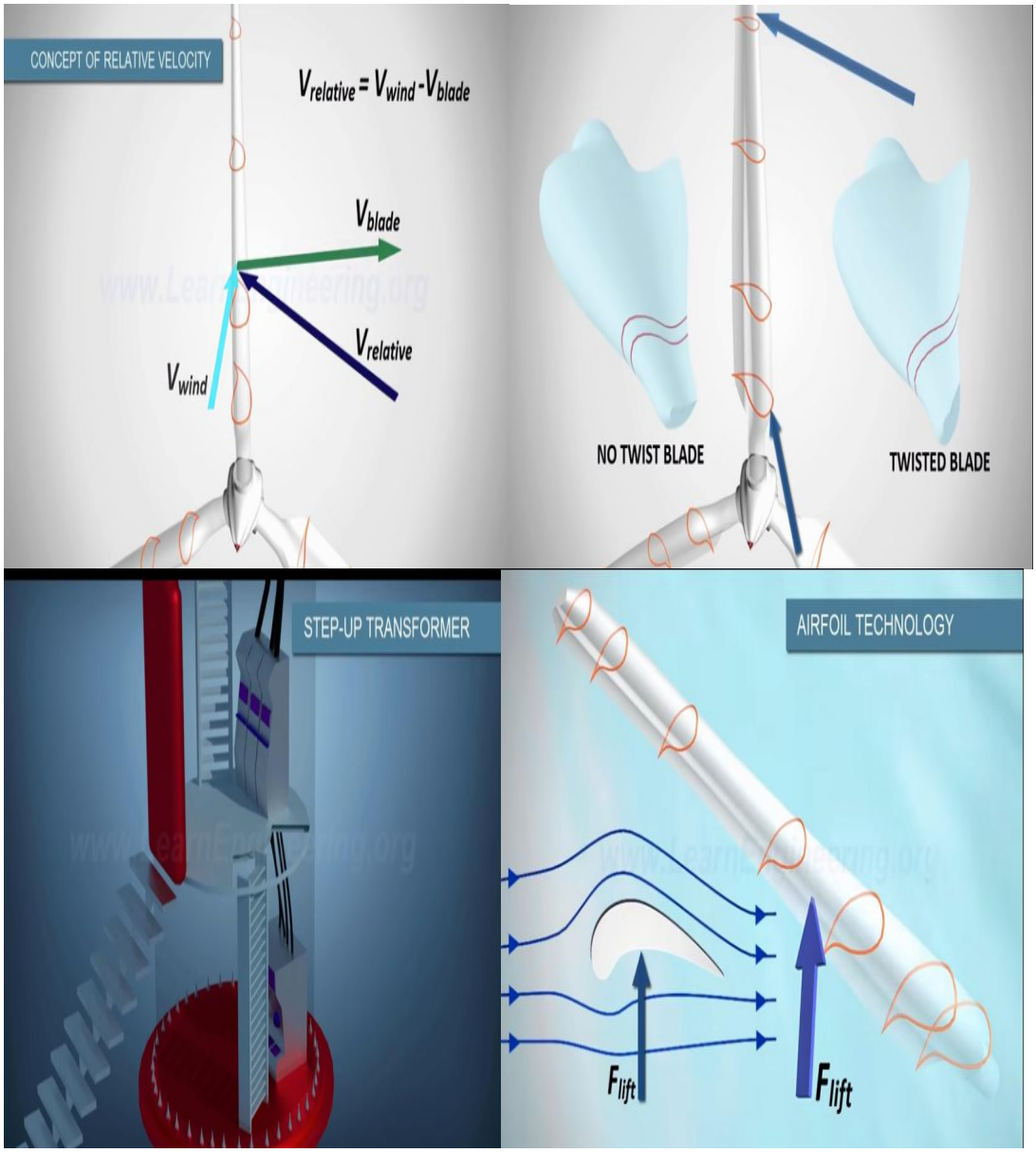

Figure 20. shows the wind turbin function

B. formulation

The wind turbine's rotor, which has radius Ri, uses speed mi to transfer wind energy to the rotor shaft. The air density, I, the swept area, Awti, and the power coefficient cpi I I all work together to calculate the power applied to the rotor.The power from the wind and the wind speed rely on one another, Vwi. The tip-speed ratio, which depends on the blade's pitch angle, is the ratio between the speed of the blade tip and the speed of the wind. I and the available power in the swept area, I = mi Ri Vwi .

The following diagram demonstrates how the turbine's rotor receives aerodynamic torque from the effective wind speed passing through it:

Taei = I + 2 mi Awti cpi (,,,)V 3 wi (1)

Whereas the relationship below comes close to becoming cpi:

cpi = (0.440.0167i)sin(i3)150.3i 0.00184(i3)i,

The drive train of the wind turbine transfers the aerodynamic torque, which is scaled down via the gearbox to the torque on the high-speed shaft, from the torque Taei on the rotor into the torque on the low-speed shaft. A wind turbine generator system (WTGS) is modeled using a two-mass drive train since this approach can accurately capture the dynamics of the system.. A two-mass drive train is used to represent a wind turbine generator system (WTGS) because it can faithfully capture the dynamic characteristics of the WTGS. The first inertia constant, Hmi, stands in for the hub, low-speed shaft, and blades, while the second inertia constant, HGi, stands in for the high-speed shaft.. rotational axis I is created by fusing the gear ratio, Ngi, of the gear box that links the shafts with the torsion stiffness, Ksi, torsion damping, Dmi, and DGi. The standard grid frequency is F.The dynamics of the shaft are denoted by the following equations: m = 1 2Hmi [Taei Ksi I Dmimi], g = 1 2HGi [Ksi I Tei DGiGi], and I = 2f(mi 1 Ngi Gi). (4) Through the stiff shaft, the generator receives mechanical power from the gear box. Tmi = Ksi I is the equation that describes the relationship between the mechanical torque and the torsional angle. (5) The stator flux transients may be disregarded in the voltage relations for modeling of fixed-speed induction generator models in power system stability studies [**J. Enslin 2003**]. The following algebraic-differential equations provide a simplified transient model of a single cage induction generator (IG) that ignores stator transients and eliminates rotor currents:

(6) E ′ qri = 1 T ′ oi E ′ qri (Xi X ′ I s = 1 2HGi [Tmi Tei]

E ′ dri, (7) E ′ dri = 1 T ′ oi E ′ dri + (Xi X ′ I

(8) Vdsi = Rsi idsi X ′ I iqsi +E ′ dri (9) Vqsi = Rsi idsi +X ′ I iqsi +E ′ qri (10), where X ′ I = Xsi + XmiXri /(Xmi + Xri), is the transient reactance, and (11) vti = q V 2 dsi +V2 qsi.

The rotor's open-circuit reactance, Xi = Xsi + Xmi,

The transient open-circuit time constant is T ′ oi = (Lri + Lmi)/Rri. The IG's terminal voltage is vti. the slip is si, Direct-axis transient voltages are denoted by E ′ dri, whereas quadrature-axis transient voltages are denoted by E ′ qri. the voltage of the d-axis stator, the voltage of the q-axis stator, Tei = Edri idsi + Eqri iqsi is the electrical torque, whereas Tmi is the mechanical torque. The stator reactance is Xsi, the rotor reactance is Xri, the magnetizing reactance is Xmi, and the stator resistance is Rsi. The IG's inertia constant is HGi, the rotor angle is I = R t 0 Gi dt, the rotor speed is Gi, the synchronous speed is s, and the d- and q-axis components of the stator current are idsi and iqsi, respectively. [**M. J. Hossain 2012**]

C. General Output:

The figure below shows few typical power curves showing the power output is limited to limit the forces on the turbine.

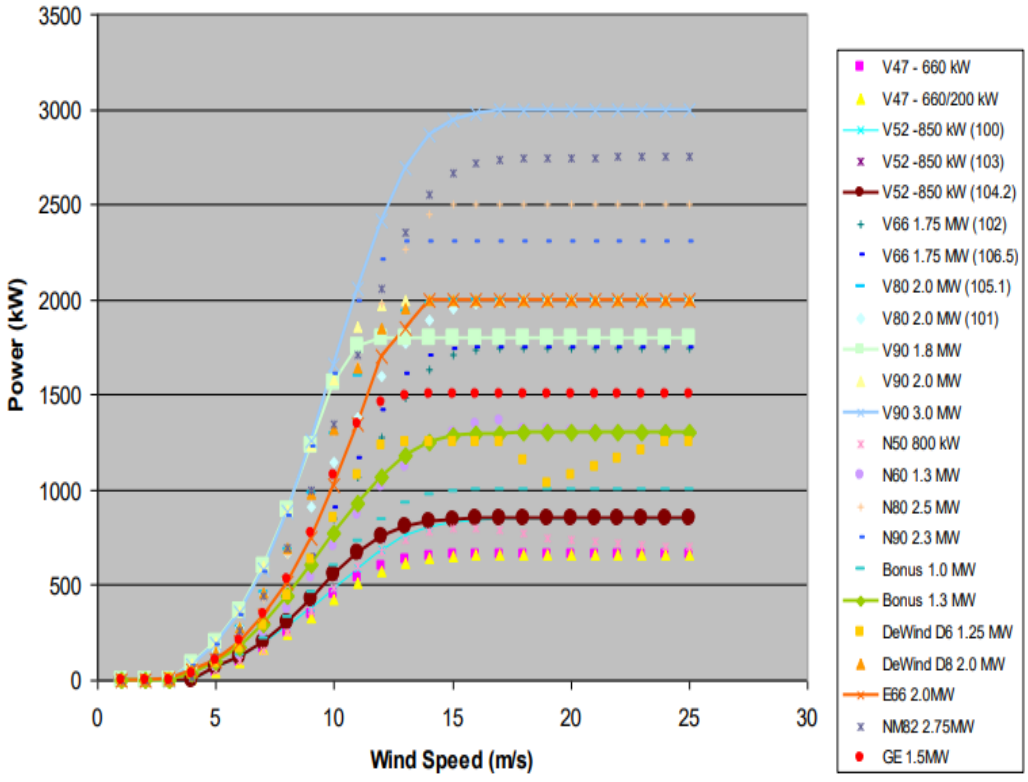

Figure 21. The amount of power extracted at various wind speeds is depicted in the image below.

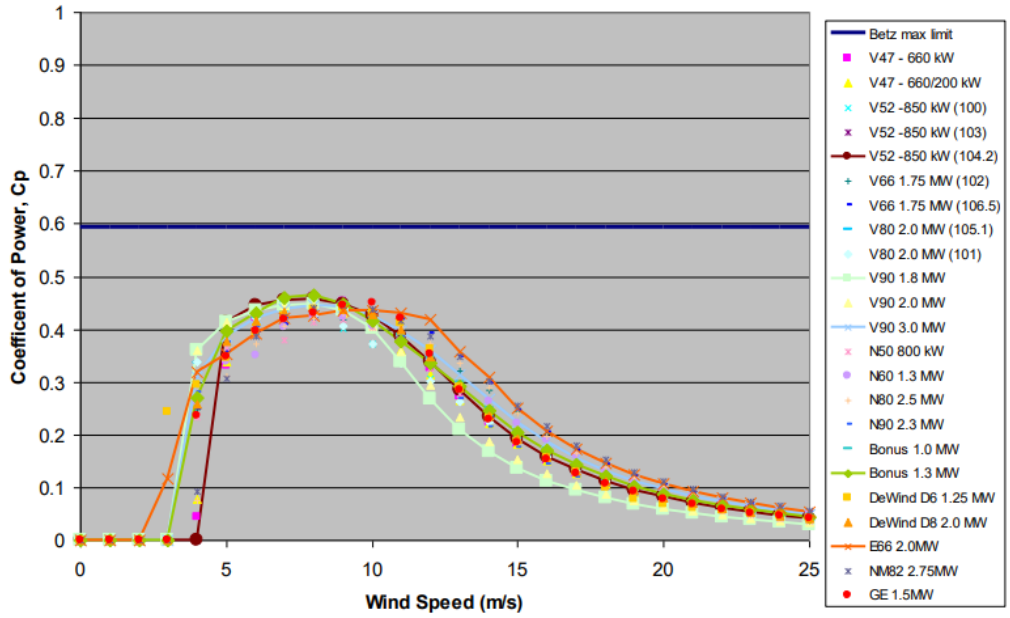

Figure 22.Coeffcient power

The practical limit is far lower than the theoretical limit and depends on the wind speed range seen at a particular site once the engineering needs to restrict the overall output power to strength and durability. The energy in the wind through Westmill's turbines is extracted at a rate of approximately 32% yearly. More often, the output of a turbine at a particular location is expressed as a capacity factor, which is the ratio of the energy produced (in a year) to the theoretical. A purely fictitious amount that would have been produced if the turbine had been operating at rated power throughout (a year). The yearly capacity factor for Westmill is roughly 21%, but it varies yearly depending on how much wind blows. With a capacity factor of 57.9% in 2005, the Burradale wind farm west of Lerwick, Shetland, holds the global record. However, due to the intense wind there, the turbines' peak power output was limited, which resulted in a lower extraction of the wind's energy than at Westmill—only around 15%.

IV. HYBRID STORAGE SYSTEM:

In isolated microgrids with erratic electrical profiles, combining a leadacid battery (ESS) with s.c is a workable solution to control the rising battery deterioration.. To increase the dependability of the power supply, a hybrid supercapacitor-battery energy storage system is used in a solar energy system. The high energy density of batteries and the high power density of supercapacitors may overlap by using the positive traits of both types of batteries and supercapacitors.The hybrid system clearly outperforms any of the component systems by exploiting each characteristic. By employing fewer batteries, the supercapacitor ensures a greener system while extending the battery's life and handling immediate peak power. Performance is significantly impacted by the energy controls used in the system to optimize the strengths and minimize the weaknesses of the energy storage devices. Utilizing supercapacitor energy is crucial when there is a sudden surge in power to prevent the power system's dependability from being jeopardized.

A. Power Filtering:

Supercapacitors are the best choice for managing the high-frequency power components of the load because to their quick dynamics, extensive cycle life, and low internal resistance. They may safeguard batteries by effectively absorbing rapid charge and discharge rates. Despite some studies showing a loss in capacitance at high operating frequencies [50]. In order to do this, here, a low pass filter is used to separate Ptot into the slowly moving Pb and the rapidly changing Psc (LPF). A first order continuous time filter with a transfer function would be the most straightforward LPF implementation.

H(s) is equal to 1/(1 + T.S) (1) when T is taken into account as the time constant. The greater the time constant, even if it does need more supercapacitor capacity, the better the filtering; but, if it is too high, their capacity may be rapidly depleted, making them unusable for lengthy periods of time.

Since high-order filters often perform better at reducing high-frequency sounds,they've been utilized in the literature to power filter ESS [24,51]. Depending on the properties of each impulse response function's temporal domain, there are two basic kinds of digital filters: finite impulse response (FIR) filters and infinite impulse response (IIR) filters. Contrary to FIR filters, high-order IIR filters often have convergence and stability problems. which don't have feedback loops and have little phase distortion [51–53].

Consequently, a FIR represented in the z-domain is the second one option taken into consideration in this research.

$$H(z) = \sum_{n=0}^{N-1} h[n] z^{-n} \quad (2)$$

$$h[n] = h_d[n]\omega[n] = \frac{sin(n\omega_c)}{n\pi}\omega[n] \quad (3)$$

When a window function is represented by ω[n]. To extract the FIR coefficients, the low-pass infinite pulse is reduced using the window function. The cut-off frequency ωc and filter length N serve as the FIR filter's design parameters. The group delay, which is inversely proportional to the window N, is an essential characteristic of a high-order FIR filter [52]. With a longer group delay, high-length windows produce greater low-pass filtering performance. Supercapacitors must compensate for power lags caused by these delays, which can occasionally result in power oscillations and subpar performance. A precise balance must be struck between the filtering effect and group delay when choosing the FIR filter length and cutoff frequency.

1. Supercapacitor Voltage Limitation

The strong coupling between the stored energy and the supercapacitors causes large voltage variations during normal operation: for a supercapacitor to completely charge, the voltage must reach its nominal value; for a supercapacitor to effectively discharge, the voltage must decrease to its lowest point. However, In order to take into consideration the structural requirements, this fluctuation must adhere to the established safety limitations VSC,min VSC,max. [**AYŞE KÜBRA 2021**] ssc properties and power converter input voltage restrictions. the sc module used in this case study should be considered [**T. M. Gür 2018**]. To deliver the nominal

maximum voltage, six batteries are linked in series. The nominal maximum voltage VSC,max is set at 16 V and the nominal lowest voltage VSC,min is chosen to be 8 V; a direct current/direct current converter must be employed to increase the voltage by up to three times to get the necessary 24 V.. Conduction and switching losses for these converters increase at conversion ratios greater than three, according to historical experience [**W.-P. Schill 2018**], It might result in a power converter that isn't able to step up the voltage, inefficient functioning, or both. The percentage of the supercapacitor ESC's usable energy capacity correlates to this voltage range.

$$E_{SC} = \frac{\frac{1}{2}CV_{SC,max}^2 - \frac{1}{2}CV_{SC,min}^2}{\frac{1}{2}CV_{SC,max}^2} = \frac{16^2 - 8^2}{16^2} = 75\%$$

Given the cheap and basic power converter employed, using 75% of the available energy is quite acceptable. These restrictions are imposed using the supercapacitor limiting mechanism. By changing battery power Pb via a signal called a PSC, the main objective is to fix any voltage breaches. PSC will be 0 when a supercapacitor is operating within its limits. However, the discharge of the supercapacitor will produce positive or negative values, respectively, when the upper or lower boundaries of the supercapacitor's voltage are passed (need to charge). Two PI controllers are used to do this, each of which controls close to one of the two voltage limits and has the essential saturation limits and anti-windup characteristics. When the voltage is within the safe range, both PI controllers are pushed to their zero saturation limits and produce zero PSC.The higher PI controller engages while the lower controller is kept at zero when VSC > VSC,max, bringing the v back to VSCm. When VSC VSC,min occurs, the opposite occurs and the lower PI controller lowers the voltage back into the safe range. The anti-windup mechanism, which allows the controllers to "unstick" from saturation as soon as the voltage surpasses acceptable limits, is a crucial part of this control technique. [**W.-P. Schill 2018**]

2. Battery Degradation Model

In order to assess how hybridization may affect battery life, a novel lead-acid battery degradation model is provided in this section.This cycle-counting technique accounts for the cumulative damage caused by the two primary stressors—battery temperature and the DoD. Most traditional models investigate these aspects independently and concentrate on medium and deep discharge cycles, or DoD >

10%, while ignoring minute changes in the SoC, or microcycles.The ESS, however, typically experiences irregular charging and discharging patterns in small-scale PV microgrids that include multiple microcycles and rapidly changing currents, which, as a result of temperature and DoD, significantly affect battery life. This study emphasizes how critical it is in these situations to use high-resolution time series that enable precise measurement of both impacts and, therefore, battery deterioration. The purpose of the following paragraphs is to provide a technique recommendation for such a degradation model that, when used with the appropriate coefficients and inputs, may be simply applied to any lead-acid battery.

3. Temperature Model

The operating temperature of the battery has a significant impact on how long it lasts. Power losses and the outside temperature Ta The most significant factor affecting battery temperature T is Ploss. The first-order low pass filter's transfer function may be used to represent their combined impact in the Laplace domain while accounting for the system's thermal inertia. $$T(s) = \frac{P_{loss} \cdot R_{th} + T_a}{1 + t_c \cdot s}$$

Rth stands for thermal resistance, while tc stands for the thermal time constant. Changes in Ta or Ploss may be won't instantly affect the battery temperature is reflected in Equation (7). Ploss stands for the battery's overall power losses. The power converter and the Ploss battery (assuming they are both set in the same cabinet) Ta is one of the model's inputs.

$$P_{loss} = P_{loss\_battery} + P_{loss\_converter}$$

The directcurrent/directcurrent converter efficiency directly determines the converter power losses. The Ploss converter is considered to be 5 percent of the actual power output at all times in this scenario since usual efficiencies range between 95 and 99 percent. [59].

B. Design

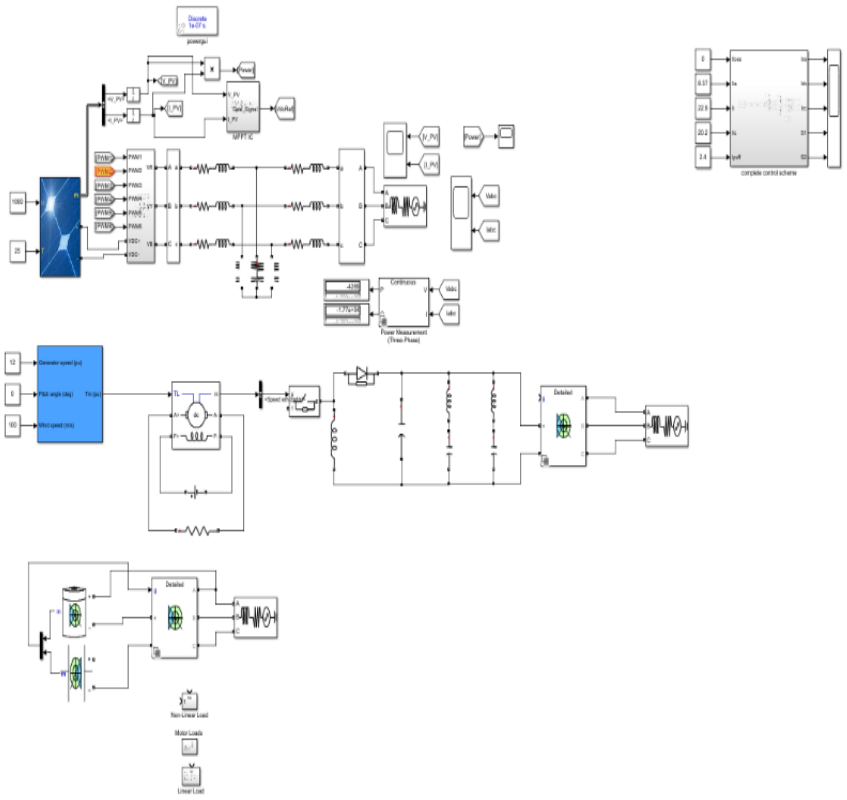

Figure 23. Full design

Full system design which is showing the pv system design , mppt ,dc load

& wind turbine parallel connected to the loads “linear ,non-linear & motor load “ which used to see the effect of the high power loads on the fluctuating of the power and as we can see the control system,

And the hybrid storage system battery and super capacitor.

We will talk about each separately

1. PV SYSTEM

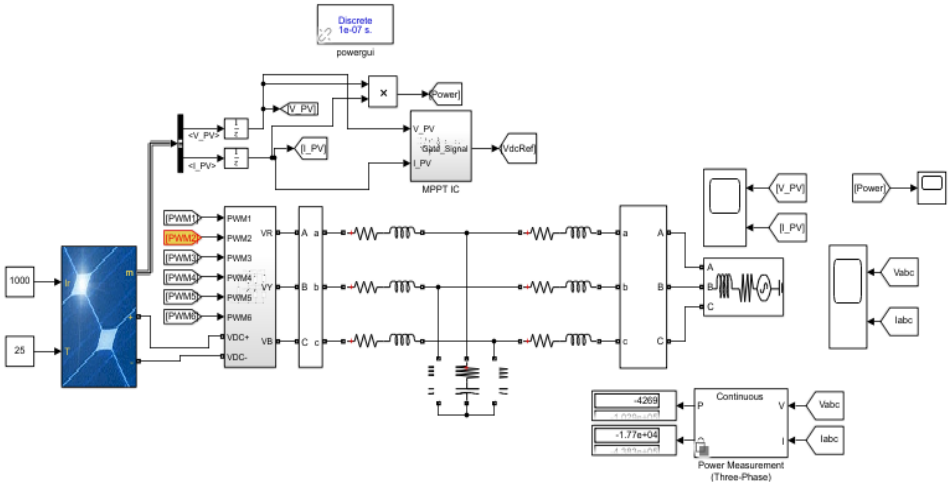

Figure 24.PV design

The maximum power point tracker (MPPT), which serves as the charge controller in this inquiry, is used to link the PV module to the DC bus in Fig. The ESSs and common DC bus are also linked to the DC load (i.e., batterybank and sc).The inverter also functions as a link between the AC and DC portions. Closed-loop control systems perform better in this aspect than open-loop systems without controllers. However, as was previously said, This study's objective is to contrast the effects of using the HBSS architecture to employing a single storage unit to the consequences of using the HBSS design. To avoid straying from the core goal of this study, This study does not look into controllers.As was noted in the literature review, many research works verify the effectiveness of hybrid battery-supercapacitor storage (HBSS) via simulations. Another example is the authors' enhanced approach, which is geared toward optimum management of sc voltage, for dealing with fluctuations in battery current in HBSS systems.As was previously said, the experimental verification of HBSS on renewable energy systems is still in its early phases. The letters Isc, Rp, Id, and Ipv, respectively, stand for the ideal current source, series resistance, parallel leakage resistance, diode voltage, and the PV module's overall output current. Eventually, the current flow reveals that the PV module is the power source. Both the battery and the supercapacitor are operating in their discharge modes concurrently with the ESSs. The KCL coupled to the analogous circuit of the first model may be written as follows:

$$IPV = Isc - Id - Ip$$

$$IL = IPV$$

$$+Ic + Ib$$

where Ib and Ic are, respectively, the battery and sc currents.

2. WIND TURBINE:

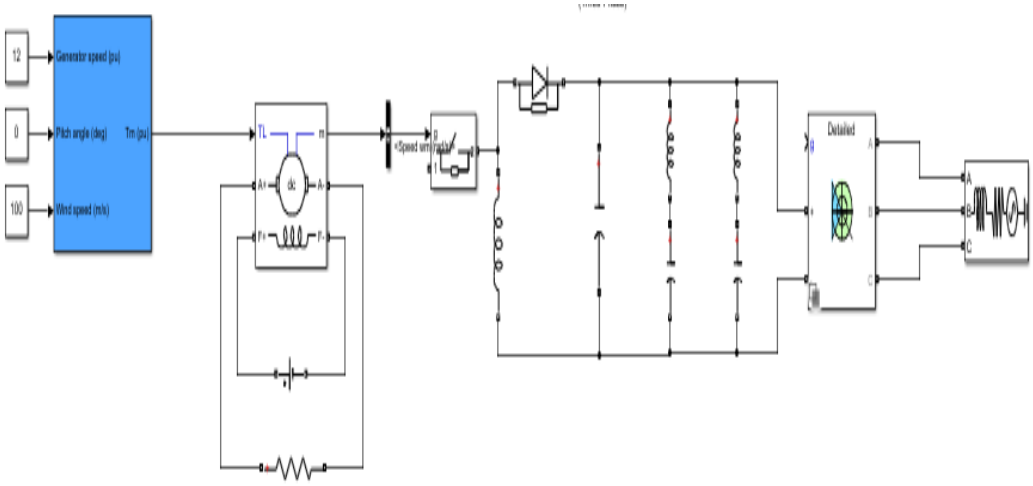

Figure 25. Wind design

According to Fig. 2, an appropriate rectifier and a charge controller link the wind turbine-generator system's three-phase output to the DC bus. The DC bus has connections for the DC load and inverter. Iw denotes the wind turbine's output current, while I - L represents the total load current on the D - C side. E. S. S. s (b. & s.c.) are discharging as a result of a wind turbine producing electricity (direction of currents). Permanent magnet synchronous generator is referred to as PMSG. It should be noted that the PMSG's dynamic model is developed from the traditional swing formulations shown in (18) and (19). (19). dm/dt = 1/ Jr (Tm) (18) e = p m (19), where p denotes the pairs of poles and T . m & T . e denote the mech. and elec. trqs, respectively; Jr is the rotor's inertia fixed ; m and e are the mech. and elec. speeds; & p is the inertia constant. In modeling and experimental experiments, A passive framework is used to link the h . s. package to the source. It is possible to extract the KCL connected to the analogous circuit as (20) or (21). When the b. and s. c. are in their charging states, the directions of current I - b and I - c will be opposing; for example, compare (20) with (21). When the amount of generation exceeds the level of demand, this circumstance will arise.

$$IL = Iw + Ib + \quad (2\ 0)$$

$$IL = Iw - Ib - \quad (2\ 1)$$

C. Control System:

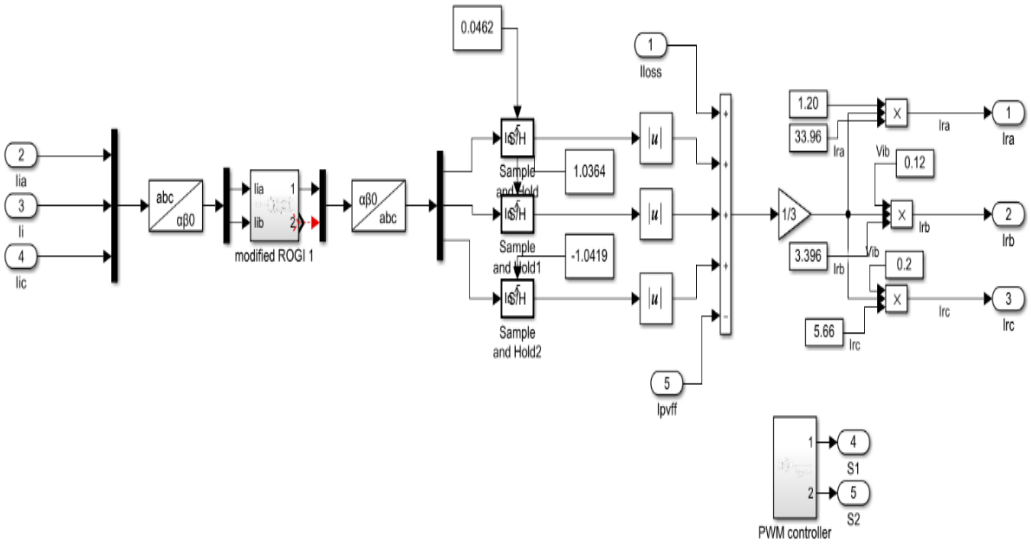

Figure 26.Control system

The whole control structure of the suggested method is shown in Figure 5.2. The load current and line voltages must be extracted using the F - C, the P - V feedforward (puff), and the unit vector template (U. V. T.). The U. V. T. Is calculated using the grid voltages at the point of common coupling, which are given as follows .

Table 3 control system formulas

$Vt=\sqrt{0.666(v_{pa}^2+v_{pb}^2+v_{pc}^2)}$ (9)	In what locations are the sensing grid voltages v pa2, v pb2, and v pc2? Grid voltages' quadrature and in-phase U.V.T components are computed using (9).
$v_{ia}=\frac{v_{pa}}{v_t}, v_{ib}=\frac{v_{pb}}{v_t}, v_{ic}=\frac{v_{pc}}{v_t}$	The U.V.T voltage is the point at which via, vib, and vic, the in-phase components of the line voltages, and Vt are. Therefore, using (10), which is denoted as follows, the quadrature U.V.T components of the line voltages are determined.
$v_{qa}=\frac{v_{ic}}{1.732}-\frac{v_{ib}}{1.732}$	To create the active power components of the load currents (ia, ib, and ic), an FC derived from the load currents is sampled and maintained in a ZCD unit with UVT quadrature components (vqa, vqb, and vqc). Using the PV feedforward term, the active power components, and the current loss components of the DC controller, the net component of the load currents is determined and is stated as follows.
$v_{qb}=\frac{1.732*v_{ia}}{2}+\frac{(v_{ib}-v_{ic})*v_{ib}}{3.464}$	The basic net component current (Inet) and the in-phase UVT components via, vib, and vic, stated as follows, are used to determine the reference currents.
$v_{qc}=-\frac{1.732*v_{ia}}{2}+\frac{(v_{ib}-v_{ic})*v_{ib}}{3.464}$	
$i_{net}=\frac{i_a+i_b+i_c-I_{pvff}}{3}$	
$i_{ra}=i_{net}*i_{ia}, \quad i_{rb}=i_{net}*i_{ib}, \; i_{rc}=i_{net}*i_{ic}$	The PWM controller receives the calculated reference currents (Ira, Irb, and Irc) and the actual grid currents (Isa, Isb, and Isc) to produce the three-phase anti-harmonic currents that are injected into the utility grid to lower harmonics and enhance power quality in the grid-integrated PV system.

D. Voltage Regulator:

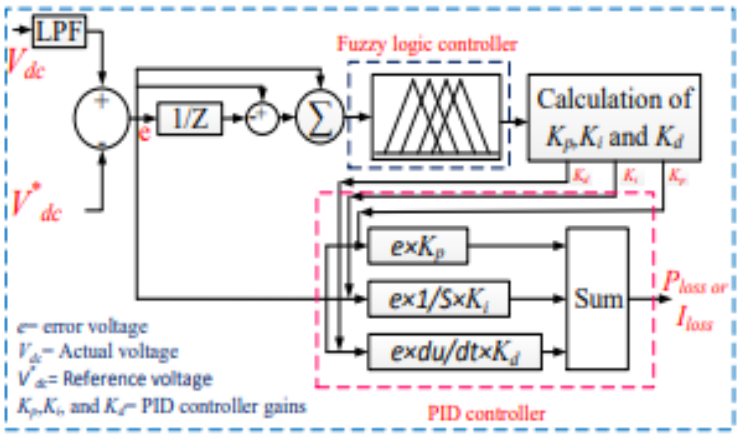

Figure 27. control system formulas

Voltage regulator

P, P - I, and P- I- D regulators have not consistently provided adequate d - c

bus voltage stabilization upon line and load transients.

To address this weakness, a fuzzy tuning adaptive PID control system was created to adaptively compute the PID gains under transient situations. Figure 5.3 displays the FLPID's control diagram. The FLPID controller's mathematical modeling is described below.

Image 5.3 an illustration of the FLPID voltage controller's schematic

Table 4 voltage regulator formulas

$G_c(S) = k_p + \frac{k_i}{s} + k_p(s)$	
$G_c(S) = k_p(1 + \frac{1}{\frac{k_p}{k_i}(s)} + \frac{k_d}{k_p}(s))$	
$u_k = k_p * e(k) + k_i.T_s \sum_{i=1}^{n} e(i) + \frac{k_d}{T_s}.e(k) - e(k-1)$	The PID controller's discrete time equivalent equation is
$k'_p = \frac{k_p - k_{p.min}}{k_{p.max} - k_{p.min}}, k'_d = \frac{k_d - k_{d.min}}{k_{d.max} - k_{d.min}}$	where uk e(k) is the error voltage obtained from the actual and reference dc voltage, is the control signal and Ts is the sampling time. The mathematical analysis of fuzzy gain scheduling for PID controller is expressed as follows,
$k'_p = \sum_{i=1}^{m} \mu_i.k'_p.i\ ,\ k'_d = \sum_{i=1}^{m} \mu_i.k'_d.i\ ,\ \alpha = \sum_{i=1}^{m} \mu_i.k'_\alpha.i$	The defuzzification yields are obtained by using the below equations,
$k_p = ((k_{pmax} - k_{pmin}).k'_p + k_{pmin})$	The PID controller's gains are obtained by using the below equations,
$k_i = \frac{k_p^2}{\alpha.k_d}, k_d((k_{dmax} - k_{dmin}).k'_d + k_{dmin})$	

E. Storage system

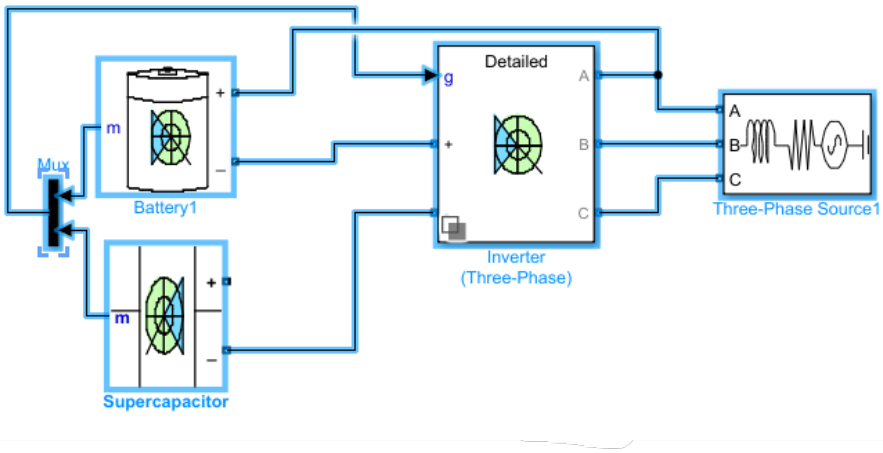

Figure 28. Storage system

Mixer “multiplexer”, battery, super capacitor, three phase source, and inverter

We have 3 phase source to measure the resistance, capacitance, loads

Connected to the multiplexer to give two input battery & supercapacitor

We need the battery to work 24 hrs. If there were no strong winds and the supercapacitor used to give a high capacity that the system can use and the inverter used to convert from dc to ac... To give us pure electricity that we can use.

Table 5 Constants Used

	Parameter	Value
PV Module	Maximum power at STC	160 W
	Open circuit voltage	22.9 V
	Short circuit current	8.37 A
	Voltage at maximum power point	20.2 V
	Current at maximum power point	7.92 A
	Number of cells per modules	32
	Operating module temperature	-40ºC to +80ºC
	Nominal operating cell temperature	47 ± 2ºC
Wind Turbine	Rated power	500 W
	Rated voltage	24 V
	Blade diameter	1.3 m
	Number of blades	5
	Rated wind speed	3 m/s

V. SIMULATION (OUTPUT)

A. Pv And Wind With One External Load “linear load”:

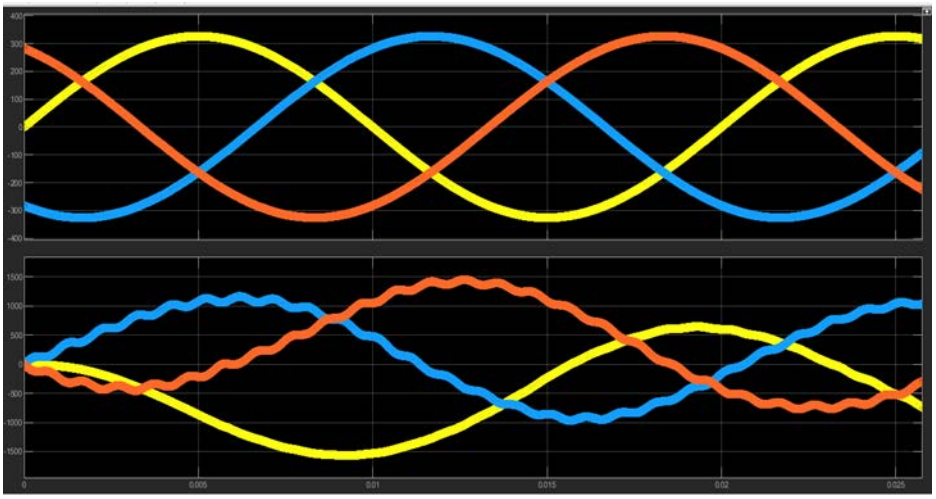

Figure 29. Current and Voltage

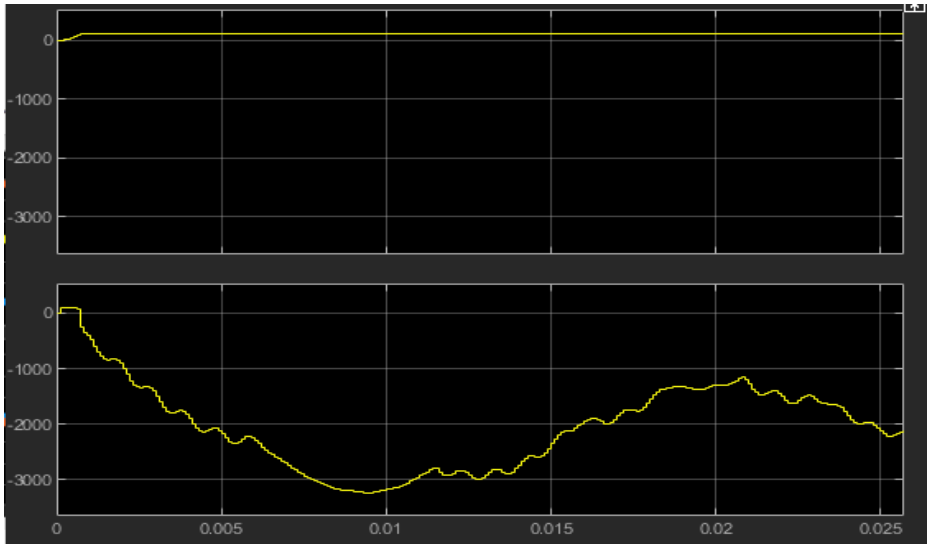

Figure 30. Curr ent and V oltage

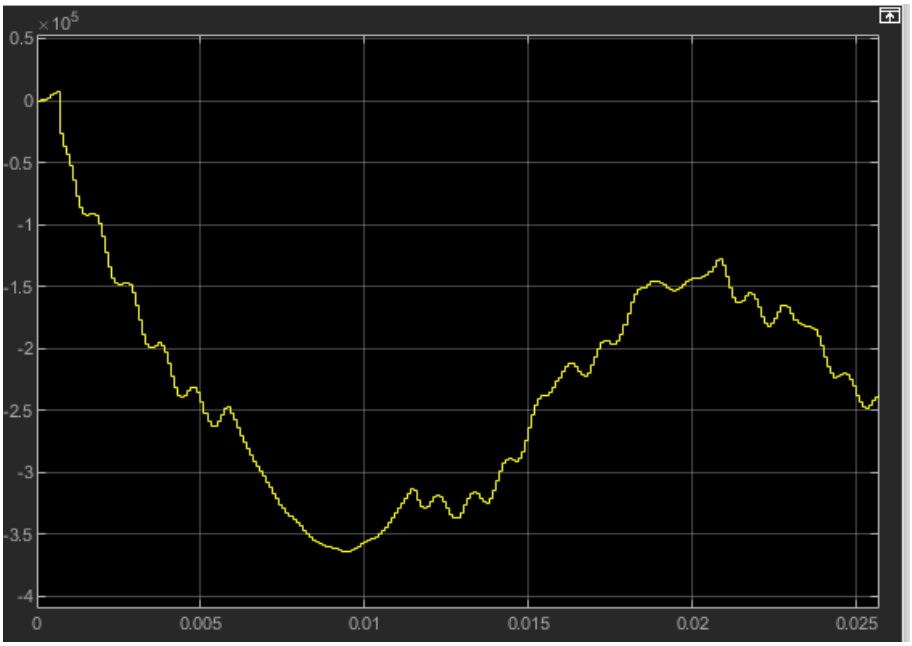

Figure 31. power of system

B. Pv And Wind With Two External Loads”linear &non linear loads”

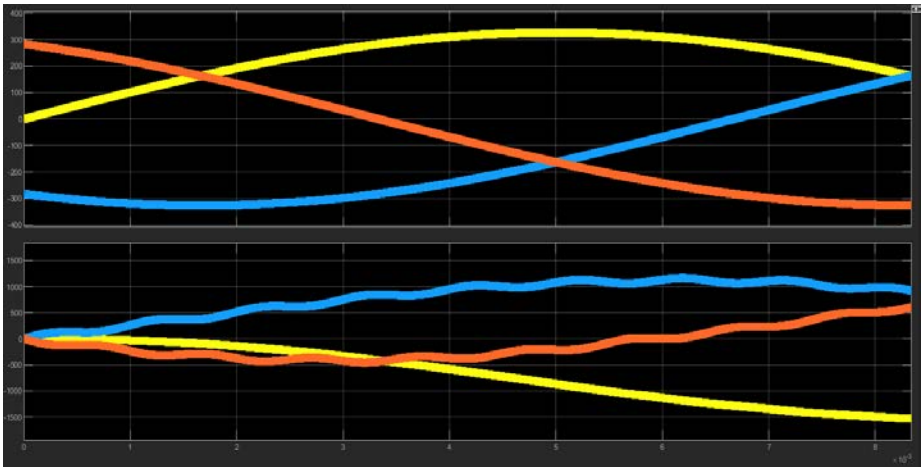

Figure 32. Current & Voltage

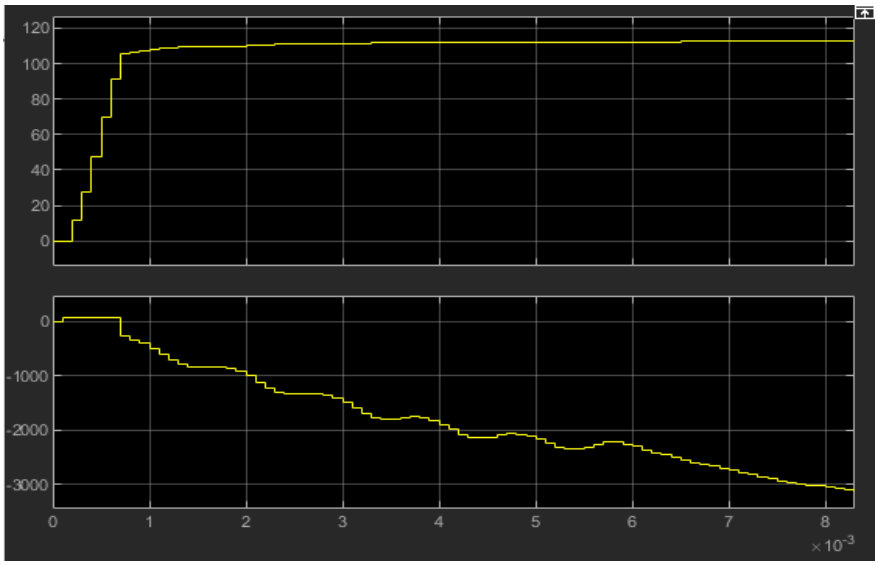

Figure 33. Current and Voltage

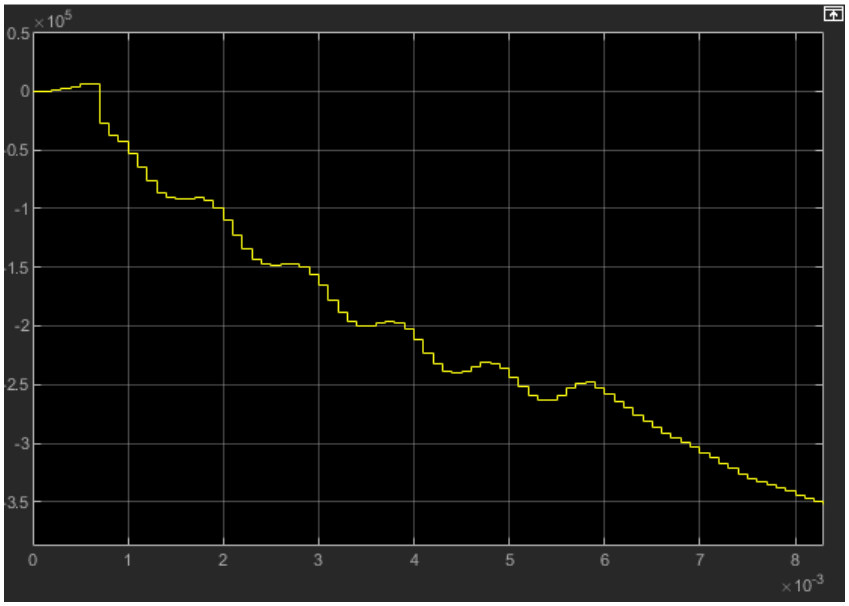

Figure 34 Power of system

C. Pv And Wind With Three External Loads”linear,non linear & motor loads”

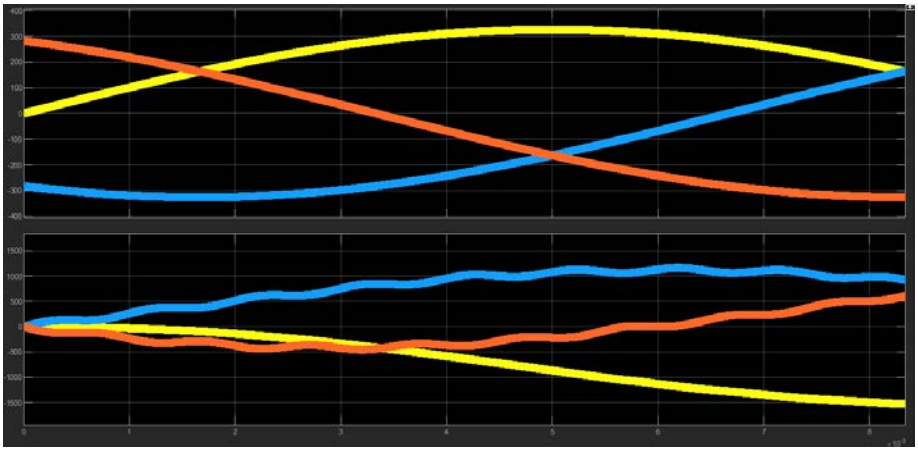

Figure 35. Current and Voltage

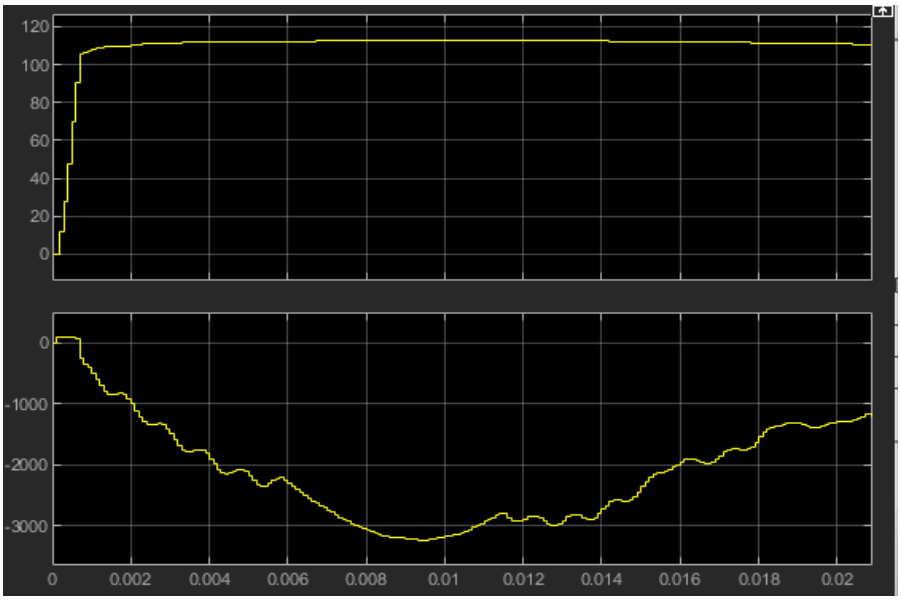

Figure 36. Curr ent and V oltage

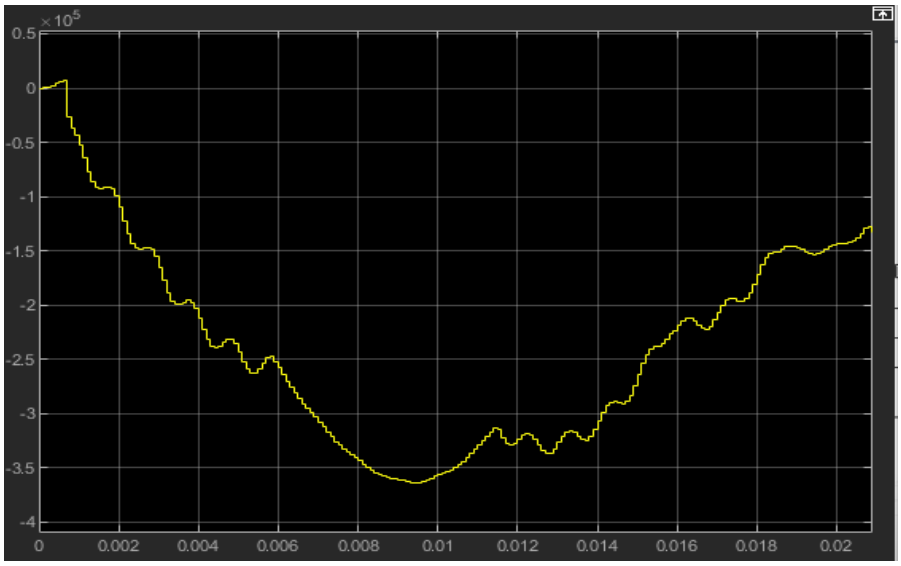

Figure 37. Power of system

D. Pv And Wind With Three External Load After Applying Supercapacitor

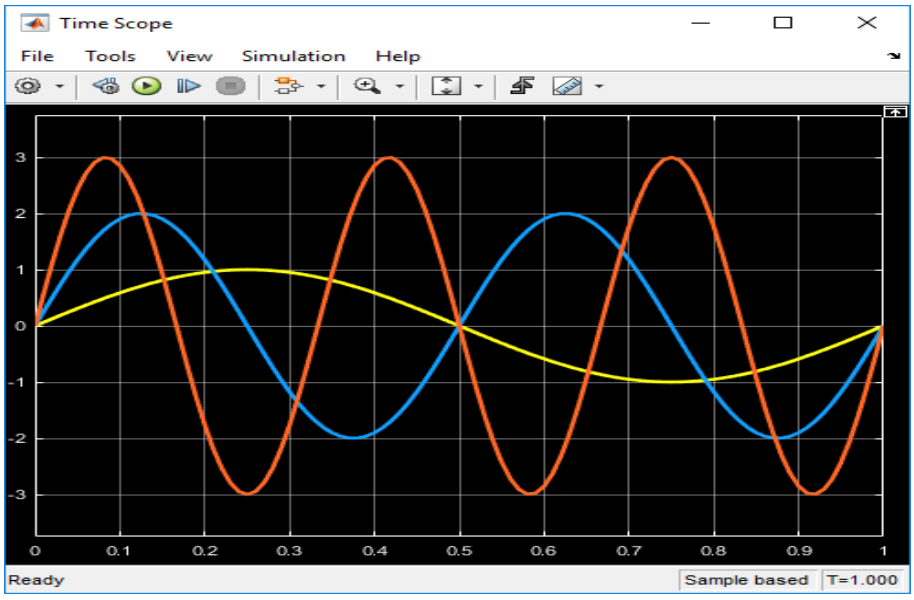

Figure 38.Current and voltage

Figure 39. Current and voltage

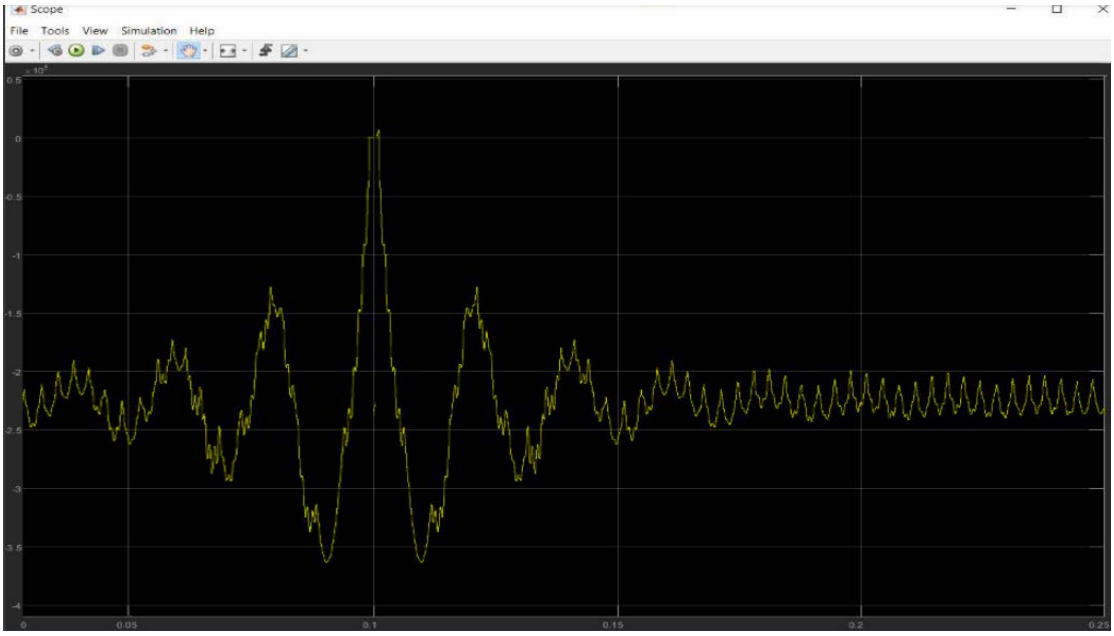

Figure 40. Power of the system

As we seen from the output curves after adding the first load with the power of the system affected by it little bit because its power wasn't that much high but when we added the both linear and nonlinear loads they affects the system power more as we seeing in fig 6.2.3 but when we add to them the motor load which have a high power we can see clearly it effect on the power it fluctuates as we see in fig 6.3.3 nonetheless, we may see the system's altering power after adding the super capacitor as we mentioned before from its characteristics that it store large electrical charge and releasing large amount of power ,reducing the reactive power which provides power from the source which reducing the current drawing that regulates

the fluctuating of the voltage of the system and take it back to the normal working function. And it’s clearly appears the sinusoid of voltage and current becomes very smooth as compare to the curves before the supercapacitor.

VI. CONCLUSION

In this study, a framework for hybrid battery-supercapacitor storage (HBSS) was created and verified. Software from Matlab/Simulink was used to get simulation-based validation. More significantly, a hybrid renewable energy system that is part of the power systems design was used for the experimental validation of the HBSS. The power and current of a PV system as well as a wind system combined while inserting the loads and after connecting the supercapacitor were shown in four distinct scenarios in the results figures.

In order to increase the supercapacitor's contribution to this framework, it must be shown that power quality has improved. Power Quality is a measurement of a supercapacitor system's ability to sustain and enhance performance after a heavy load. Voltage, current, or frequency may all be involved in a power disturbance or incident. Consumer loads, consumer power systems, or the utility are all potential sources of power interruptions. We employed a supercapacitor to feed the system and steady the power in the system to prevent fluctuations in our system during periods of heavy load.

The three high power loads that were introduced to the design have an impact on the voltage of the whole system, which is the most important conclusion that can be made from the research after confirming the final data. A super capacitor was thus installed to positively calibrate the voltage.

VII. REFRENCESS

BOOKS

WEIDONG XIAO, '**Photovoltaic Power System: Modeling, Design, and Control**'.

ALİ M. ELTAMALY, ALMOATAZ Y.ABDELAZIZ, ' **Modern Maximum Power Point Tracking Techniques for Photovoltaic Energy Systems**. Hoboken, NJ: John Wiley & Sons, 2017.

NABİL DERBEL ،QUANMİN ZHU, **'Modeling, Identification and Control Methods in Renewable Energy Systems'**. Sfax Tunsia Bristol UK, May 2018

ARTICLE

E. MOHAMMADİ, R. RASOULİNEZHAD, AND G. MOSCHOPOULOS, "**Using a supercapacitor to mitigate battery microcycles due to wind shear and tower shadow effects in wind-diesel microgrids, IEEE Trans. Smart Grid**, vol. 11, no. 5, pp. 3677-3689, Sep. 2020.

M. J. HOSSAİN, MEMBER, IEEE, H. R. Pota, M. A. Mahmud and Rodrigo A. Ramos, Senior Member, IEEE Systems Journal (Volume: 6, Issue: 1, March 2012)

A topological o opological overview of micr view of microgrids: fr ogrids: from maturity t om maturity to the futur o the future AYŞE KÜBRA ERENOĞLU SEMANUR SANCAR OZAN ERDİNÇ MUSTAFA BAĞRIYANIK Vol. 29: No. 3, Article 2 (2021)

T. M. GÜR, "**Review of electrical energy storage technologies, materials and systems: Challenges and prospects for large-scale grid storage**," Energy Environ. Sci., vol. 11, no. 10, pp. 2696–2767, Oct. 2018.

W.-P. SCHİLL, "**Electricity storage and the renewable energy transition**," Joule, vol. 4, no. 10, pp. 2059–2064, Oct. 2020.

S. KİM et al., “**A -20 to 30 dBm input power range wireless power system with a MPPT-based reconfigurable 48% efficient RF energy harvester and 82% efficient A4WP wireless power receiver with openloop delay compensation**," IEEE Trans. Power Electron., vol. 34, no. 7, pp. 6803-6817, Jul. 2019.

OTHER RESOURCES

A. ELMEHDİ, B. JOHNSON, M. ABUAGREB, AND W. PARKER, “**Analysis, modeling, and control of a stand-alone photovoltaic generation system**,” in 2016 4th International Conference on Control Engineering Information Technology (CEIT), Dec 2016

S. BHATTACHARYYA, J.M.A. MYRZİK, AND W.L. KLİNG, “**Consequences of poor power quality-an overview**,” International Universities Power Engineering Conference, Brighton, UK, Sept. 4-6, 2007, pp. 651-656.

M. J. HOSSAİN, H. R. POTA, V. UGRİNOVSKİİ, AND R. A. RAMOS, “**Excitation control for large disturbances in power systems with dynamic loads**,” in IEEE Power and Energy Society General Meeting, July 2009, pp. 1–8.

J. ENSLİN, J. KNİJP, C. JANSEN, AND P. BAUER, “**Integrated approach to network stability and wind energy technology for on-shore and offshore applications**,” in 24th International Conference for Power Electronics, Intelligent Motion and Power Quality, Nuremberg, Germany, May 2003, pp. 1–8.

RESUME

Name Surname: YAHYA ABU ATTEIEH

Education:

2013-2017 Near East University, Electrical and Electronics Engineering

2020-2022 İstanbul Aydın University, Master's Degree Electrical and Electronics Engineering

Work Experience:

2017-2020 Meedan Engineering Company

Languages:

-Arabic: Native Language

-English: Advanced

- Turkish: Intermediate

Skills:

-Communication, Teamwork, Problem Solving, Flexibility, Creativity

- Computer skills (Microsoft Office) and others